

MODELLING OF THE HEART AND PERICARDIUM AT END-DIASTOLE

BY

P.N. SHIVAKUMAR

CHI-SING MAN

SIMON W. RABKIN

IMA Preprint Series # 265

September 1986

INSTITUTE FOR MATHEMATICS AND ITS APPLICATIONS
UNIVERSITY OF MINNESOTA
514 Vincent Hall
206 Church Street S.E.
Minneapolis, Minnesota 55455

- # Author(s) Title
- 120 D.R.J. Chillingworth, Three Introductory Lectures on Differential Topology and its Applications
- 121 Giorgio Vergara Caffarelli, Green's Formulas for Linearized Problems with Live Loads
- 122 F. Chiarenza and M. Garofalo, Unique Continuation for Nonnegative Solutions of Schrödinger Operators
- 123 J.L. Ericksen, Constitutive Theory for some Constrained Elastic Crystals
- 124 Minoru Murata, Positive solutions of Schrödinger Equations
- 125 John Maddocks and Gareth P. Parry, A Model for Twinning
- 126 M. Kaneko and M. Wooders, The Core of a Game with a Continuum of Players and Finite Coalitions: Nonemptiness with Bounded Sizes of Coalitions
- 127 William Zame, Equilibria in Production Economies with an Infinite Dimensional Commodity Space
- 128 Myrna Holtz Wooders, A Tiebout Theorem
- 129 Abstracts for the Workshop on Theory and Applications of Liquid Crystals
- 130 Yoshikazu Giga, A Remark on A Priori Bounds for Global Solutions of Semilinear Heat Equations
- 131 M. Chipot and G. Vergara-Caffarelli, The N-Membranes Problem
- 132 P.-L. Lions and P.-E. Souganidis, Differential Games and Directional Derivatives of Viscosity Solutions of Isaacs' Equations II
- 133 G. Capriz and P. Glavine, On Virtual Effects During Diffusion of a Dispersed Medium in a Suspension
- 134 Fall Quarter Seminar Abstracts
- 135 Umberto Mosco, Wiener Criterion and Potential Estimates for the Obstacle Problem
- 136 Chi-Sing Man, Dynamic Admissible States, Negative Absolute Temperature, and the Entropy Maximum Principle
- 137 Abstracts for the Workshop on Oscillation Theory, Computation, and Methods of Compensated Compactness
- 138 Arle Leizarowitz, Tracking Nonperiodic Trajectories with the Overtaking Criterion
- 139 Arle Leizarowitz, Convex Sets in R^n as Affine Images of some Fixed Set in R^n
- 140 Arle Leizarowitz, Stochastic Tracking with the Overtaking Criterion
- 141 Abstracts from the Workshop on Amorphous Polymers and Non-Newtonian Fluids
- 142 Winter Quarter Seminar Abstracts
- 143 D.G. Aronson and J.L. Vazquez, The Porous Medium Equation as a Finite-speed Approximation to a Hamilton-Jacobi Equation
- 144 E. Sanchez-Palencia and H. Weinberger, On the Edge Singularities of a Composite Conducting Medium
- 145 Jon C. Luke, Soliton Solutions in a Class of Fully Discrete Nonlinear Wave Equations
- 146 Chi-Sing Man and H. Cohen, A Coordinate-Free Approach to the Kinematics of Membranes
- 147 J.L. Lions, Asymptotic Problems in Distributed Systems
- 148 Reiner Lauterbach, An Example of Symmetry Breaking with Submaximal Isotropy Subgroup
- 149 Abstracts from the Workshop on Metastability and Incompletely Posed Problems
- 150 B. Bozar-Karakiewicz and Jerry Bona, Wave-dominated Shelves: A Model of Sand-Ridge Formation by Progressive, Infragravity Waves
- 151 Abstracts from the Workshop on Dynamical Problems in Continuum Physics
- 152 V.I. Olliker, The problem of Embedding S^n into R^{n+1} with Prescribed Gauss
- 153 R. Batra, The force on a Lattice Defect in an Elastic Body
- 154 J. Fleckinger and Michael Lepidus, Eigenvalues of Elliptic Boundary Value Problems with and indefinite Weight Function
- 155 R. Kohn and M. Vogelius, Thin Plates with Rapidly Varying Thickness, and Their relation to Structural Optimization
- 156 M. Gurtin, Some Results and Conjectures in the Gradient Theory of Phase Transitions
- 157 A. Novick-Cohen, Energy Methods for the Cahn-Hilliard Equation
- 158 M. Biroli and U. Mosco, Wiener Estimates for Parabolic Obstacle Problems
- 159 E. Bennett and M. Zame, Prices and Bargaining in Cooperative Games
- 160 M.A. Harris and Y. Sibuya, The n -th Roots of Solutions of Linear Ordinary Differential Equations
- 161 Millard F. Beatty, Some Dynamical Problems in Continuum Physics
- 162 P. Bauman and D. Phillips, Large-Time Behavior of Solutions to a Scalar Conservation Law in Several Space Dimensions
- 163 A. Novick-Cohen, Interfacial Instabilities in Directional Solidification of Dilute Binary Alloys: The Kuramoto-Sivashinsky Equation.
- 164 H.F. Weinberger, On Metastable Patterns in Parabolic Systems
- 165 D. Arnold and R.S. Falk, Continuous Dependence on the Elastic Coefficients for a Class of Anisotropic Materials
- 166 I.-J. Bekelman, The Boundary Value Problems for Non-linear Elliptic Equation and the Maximum Principle for Euler-Lagrange Equations
- 167 Ingo Müller, Gases and Rubbers
- 168 Ingo Müller, Pseudoelasticity in Shape Memory Alloys - an Extreme Case of Thermoelasticity
- 169 Luis Magalhães, Persistence and Smoothness of Hyperbolic Invariant Manifolds for Functional Differential Equations
- 170 A. Damiljan and M. Vogelius, Homogenization Limits of the Equations of Elasticity in Thin Domains
- 171 H.C. Simpson and S.J. Spector, On Hadamard Stability in Finite Elasticity
- 172 J.L. Vazquez and G. Yarur, Isolated Singularities of the Solutions of the Schrödinger Equation with a Radial Potential
- 173 G. Dal Maso and U. Mosco, Wiener's Criterion and L^1 -Convergence
- 174 John H. Maddocks, Stability and Folds
- 175 R. Hardt and D. Kinderlehrer, Existence and Partial Regularity of Static Liquid Crystal Configurations
- 176 M. Nerukar, Construction of Smooth Ergodic Cocycles for Systems with Fast Periodic Approximations
- 177 J.L. Ericksen, Stable Equilibrium Configurations of Elastic Crystals
- 178 Patricio Aviles, Local Behavior of Solutions of Some Elliptic Equations
- 179 S.-N. Chow and R. Lauterbach, A Bifurcation Theorem for Critical Points of Variational Problems
- 180 R. Pego, Phase Transitions: Stability and Admissibility in One Dimensional Nonlinear Viscoelasticity
- 181 Mariano Glaquinta, Quadratic Functions and Partial Regularity
- 182 J. Bona, Fully Discrete Galerkin Methods for the Korteweg De Vries Equation
- 183 J. Maddocks and J. Keller, Mechanics of Robes
- 184 F. Bernis, Qualitative Properties for some nonlinear higher order
- 185 F. Bernis, Finite Speed of Propagation and Asymptotic Rates for some Nonlinear Higher Order Parabolic Equations with Absorption
- 186 S. Reichelstein and S. Reiter, Game Forms with Minimal Strategy Spaces
- 187 T. Ding, An Answer to Littlewood's Problem on Boundedness
- 188 J. Rubinstein and R. Mauri, Dispersion and Convection in Periodic Media
- 189 W.H. Fleming and P.E. Souganidis, Asymptotic Series and the Method of Vanishing Viscosity
- 190 H. Beltrao Da Veiga, Existence and Asymptotic Behavior for Strong Solutions of Navier-Stokes Equations in the Whole Space
- 191 L.A. Caffarelli, J.L. Vazquez, and M.L. Wolanski, Lipschitz Continuity of Solutions and Interfaces of the N-Dimensional Porous Medium Equation
- 192 R. Johnson, m-Functions and Floquet Exponents for Linear Differential System:
- 193 F.V. Atkinson and L.A. Peletier, Ground States and Dirichlet Problems for $-\Delta = F(U)$ in R^n
- 194 G. Dal Maso, U. Mosco, The Wiener Modulus of a Radial Measure
- 195 H. A. Levine and H.F. Weinberger, Inequalities between Dirichlet and Neumann Eigenvalues
- 196 J. Rubinstein, On the Macroscopic Description of Slow Viscous Flow Past a Random Array of Spheres
- 197 G. Dal Maso and U. Mosco, Wiener Criteria and Energy Decay for Relaxed Dirichlet Problems

MODELLING OF THE HEART AND PERICARDIUM AT END-DIASTOLE

by

P.N. Shivakumar
Department of Applied Mathematics
The University of Manitoba
Winnipeg, Manitoba R3T 2N2
Canada

Chi-Sing Man*
Department of Mathematics
University of Kentucky
Lexington, Kentucky 40506-0027
U.S.A.

Simon W. Rabkin
Faculty of Medicine
University of British Columbia
Shaughnessy Hospital
Vancouver, British Columbia V6H 3N1
Canada

August, 1986

*Author to whom correspondence should be addressed.

ABSTRACT

Herein we develop a model of the left ventricle and pericardium at end-diastole. In our model the left ventricle at end-diastole assumes the shape of a spherical thick-walled shell, and the pericardium is a spherical membrane concentric with it. We assume that both the thick-walled shell and the membrane are homogeneous and are composed of incompressible, isotropic and Cauchy-elastic materials. Two empirical stress-strain relations obtained from biaxial uniform-extension tests on the two materials, respectively, will suffice to specify our model. The model gave good fit to experimental data from excised canine ventricles and to pericardium data from closed chest, anaesthetized dogs. Three empirical stress-strain relations were tried in the data-fitting. The "exponential law" gave the best results.

INTRODUCTION

The heart is a thick-walled muscle enclosed in a loose-fitting sac or pericardium, which is a thin membrane but much stiffer than the heart muscle. The small space between the pericardium and the heart is filled by the pericardial fluid.

Intracardiac pressures and volumes are influenced by the pericardium (cf. Pegram et al. (1975), Glantz et al. (1978), Shirato et al. (1978), Kanazawa et al. (1983)), although the pericardium probably has little effect in the normal man at rest. When the heart is larger during exercise, the pericardium will assume a bigger role because cardiac dilatation must occur against the confinement of the much stiffer pericardium. Pericardial disease is an important clinical problem. Excessive fluid in the pericardial sac (pericardial effusion) can lead to the potentially fatal condition of cardiac tamponade. Some inflammations of the pericardium can result in constriction of the heart. Understanding quantitatively the effects of the pericardium on intracardiac pressures and volumes would allow a better assessment of the severity of myocardial diseases and the effect of pericardial disease on the heart.

Unfortunately, although cardiologists routinely measure intracardiac pressures and volumes, they are as yet unable routinely to assess the role of the pericardium quantitatively. A mathematical model which captures and describes quantitatively the role of pericardium in cardiac mechanics will have important clinical applications. In this paper

we shall develop a model of the left ventricle at end-diastole that includes the pericardium in the modelling. Many earlier models of the left ventricle did not include the pericardium (see, e.g., Mirsky (1973), Demiray (1976)). Vito (1979) studied "the effects of the pericardium on a mechanical model of the heart". Our study differs from Vito's in two ways:

(1.) Vito studied experimentally the one-dimensional elastic response of excised dog pericardium in tension tests, used his data in the modelling, and concluded that his model "shows the effects of pericardial thickness changes on pressures in the heart to be significant". The relationship between his static model and the pumping heart was not examined. Similarity to the models of Mirsky (1973) and Demiray (1976) was mentioned. However, both Mirsky and Demiray were interested in the elastic properties of the left ventricle. They tested their model by using experimental data of Spotnitz et al. (1966), which were obtained from excised canine left ventricles without pericardium. Our model refers to the left ventricle and pericardium at end-diastole. Below we shall use our model to fit data obtained from closed chest, anaesthetized dogs.

(2.) Although our model and Vito's model are identical in geometry, our analysis differs from his in mechanics. Vito assumed that the left ventricle and the pericardium were homogeneous and composed of incompressible isotropic hyperelastic materials. For each material he postulated a stored-energy function with two material parameters. For the stored-energy function of the pericardial material he estimated the values of its

parameters by fitting his data of uniaxial tension tests on canine pericardium. As we shall explain below, as far as mechanics goes, relevant data are those of uniaxial compression or uniform biaxial extension tests. A stored-energy function which gives good fit to data of uniaxial tension tests need not deliver correct response for uniaxial compression tests. In this sense there is a logical gap in Vito's analysis. Moreover, because of the geometry of the modelling, stored-energy functions are not essential in the mechanical analysis. Indeed in our model we shall assume that the left ventricle and the pericardium be Cauchy elastic instead of hyperelastic. Cf. Truesdell and Noll (1965), §43 and §82, for the distinction between hyperelasticity and the more general Cauchy elasticity.

MATHEMATICAL MODELLING

The following model refers to the heart at end-diastole. Pressures and diameters, if not specified otherwise, are end-diastolic pressures and diameters.

We model the left ventricle as a thick-walled spherical shell, which is an approximation adopted in many previous studies. We treat the pericardium as a spherical membrane concentric with the thick-walled shell. We assume that the membrane and the thick-walled shell are homogeneous and composed of different incompressible isotropic Cauchy-elastic materials. Inside the thick-walled shell and between it and the spherical membrane are two different fluids. We assume that at end-diastole the system of

fluids, spherical membrane and thick-walled shell is at static equilibrium.

Our goal in this section can be paraphrased as follows: to derive equations that describe the effects of changes in pericardial end-diastolic pressure (i.e., pressure of fluid enclosed between the spherical membrane and the thick-walled shell at the end of cardiac diastole) on the dimensions of the spherical membrane and thick-walled shell. To this end we shall consider various equilibrium configurations of the system at end-diastole, in which the pericardial pressure and left ventricular pressure are variables.

The problem under consideration requires large deformation analysis. Because existing experimental data on the large deformation of soft biological tissues are obtained mainly from uniaxial and uniform biaxial tests, much effort in the past has been spent in attempting to arrive at a stored-energy function from the restricted experimental data. For our present problem, however, such a generalization is unnecessary. Indeed we need not assume that a stored-energy function exists at all. In other words, it suffices to assume that the biological tissues in question are Cauchy elastic rather than hyperelastic. Moreover, for the model at hand, two empirical functions will suffice to specify our model completely; these functions are those which fit stress-strain data of uniaxial compression or biaxial uniform-extension tests on the two materials that constitute the thick-walled shell and the spherical membrane, respectively. (Under our constitutive assumptions the information content of biaxial uniform-extension tests is identical to that of uniaxial compression tests.

Cf. the derivation of Eq. (13) below.)

The most handy stress-strain data on soft biological tissues are those of uniaxial tension tests. For our modelling of the thick-walled shell we need to know a function

$$\sigma = f(\epsilon; \alpha_1, \dots, \alpha_\ell) \quad (1)$$

which will fit stress-strain data of uniaxial compression tests on the material of the shell. Here σ is the nominal engineering stress or Lagrangian stress, ϵ is the conventional engineering strain (i.e., the change in length per unit original length), and $\alpha_1, \dots, \alpha_\ell$ are material parameters. Moreover, we have assumed that the configuration defined by $\epsilon = 0$ is identical to that of a material point in the thick-walled shell when the shell is at ease (i.e., unstressed) before inflation. For our intended applications the material parameters $\alpha_1, \dots, \alpha_\ell$ will be determined in vivo. Thence we need to know only the functional form of Eq. (1), which can be inferred from biaxial uniform-extension tests on excised pericardia and ventricle-wall muscles of animals. Results of uniaxial tension tests are also helpful in providing possible forms of Eq. (1), as we shall see below.

Since we have assumed that the material of the thick-walled shell is incompressible, isotropic and Cauchy elastic, its constitutive equation has the representation (cf. Truesdell and Noll (1965), Eq. (49.5))

$$\underline{T} = -p\underline{I} + \beta_1\underline{B} + \beta_{-1}\underline{B}^{-1}; \quad (2)$$

here \underline{T} is the Cauchy stress, p is the indeterminate pressure due to incompressibility, \underline{B} is the left Cauchy-Green tensor, β_1 and β_{-1} are symmetric scalar functions of the eigenvalues of \underline{B} . Consider a uniaxial compression test on a specimen that obeys Eq. (1). Suppose a Cartesian coordinate system has been chosen. Let 1- be the direction of compression on the specimen and let λ denote the stretch ratio in the 2- and 3- directions. For a typical material point in the specimen the left Cauchy-Green tensor has the form

$$\underline{B} = \begin{bmatrix} \lambda^{-4} & 0 & 0 \\ 0 & \lambda^2 & 0 \\ 0 & 0 & \lambda^2 \end{bmatrix}, \quad (3)$$

and the Cauchy stress is given by

$$\underline{T} = \begin{bmatrix} T_{11} & 0 & 0 \\ 0 & 0 & 0 \\ 0 & 0 & 0 \end{bmatrix}. \quad (4)$$

For a compression test, $\lambda > 1$ and $T_{11} < 0$. It follows from Eqs. (2), (3) and (4) that

$$\begin{aligned}
 T_{11} &= -p + \beta_1(\lambda^{-4}, \lambda^2, \lambda^2)\lambda^{-4} + \beta_{-1}(\lambda^{-4}, \lambda^2, \lambda^2)\lambda^4 \\
 &= -p + \hat{\beta}_1(\lambda)\lambda^{-4} + \hat{\beta}_{-1}(\lambda)\lambda^4, \\
 T_{22} &= T_{33} = -p + \hat{\beta}_1\lambda^2 + \hat{\beta}_{-1}\lambda^{-2} = 0,
 \end{aligned}
 \tag{5}$$

where $\hat{\beta}_j(\lambda) \equiv \beta_j(\lambda^{-4}, \lambda^2, \lambda^2)$ for $j = 1$ and $j = -1$. On the other hand, by Eq. (1)

$$\begin{aligned}
 T_{11} &= \lambda^{-2}\sigma = \lambda^{-2}f(\epsilon; \alpha_1, \dots, \alpha_\ell) \\
 &= \lambda^{-2}f(\lambda^{-2} - 1; \alpha_1, \dots, \alpha_\ell).
 \end{aligned}
 \tag{6}$$

Thence we deduce that

$$\begin{aligned}
 T_{11} - T_{22} &= \hat{\beta}_1(\lambda)(\lambda^{-4} - \lambda^2) + \hat{\beta}_{-1}(\lambda)(\lambda^4 - \lambda^{-2}) \\
 &= \lambda^{-2}f(\lambda^{-2} - 1; \alpha_1, \dots, \alpha_\ell).
 \end{aligned}
 \tag{7}$$

Now consider a dilatation of the thick-walled spherical shell in question. The shell is considered to remain spherical after the deformation, and we assume that it is at static equilibrium in its current configuration under the given internal and outside pressures. We shall use spherical coordinates (r, θ, ϕ) to denote the current position of a material point of the shell after dilatation. Let R_i and R_o be the original inner and outer radii of the spherical shell when it is at ease.

Let r_i and r_o be the inner and outer radii after the dilatation. Let r be the radius after dilatation of the spherical surface whose original radius is R . For a material point X on this surface the left Cauchy-Green tensor is given under spherical coordinates by

$$\underline{B} = \begin{bmatrix} \lambda^{-4} & 0 & 0 \\ 0 & \lambda^2 & 0 \\ 0 & 0 & \lambda^2 \end{bmatrix}, \quad (8)$$

where $\lambda = r/R$; here $\lambda > 1$ for a dilatation. It follows from Eq. (2) that under spherical coordinates the physical components of the Cauchy stress tensor \underline{T} at X are given by the expressions

$$\begin{aligned} T_{rr} &= -p + \hat{\beta}_1(\lambda)\lambda^{-4} + \hat{\beta}_{-1}(\lambda)\lambda^4, \\ T_{\theta\theta} &= T_{\phi\phi} = -p + \hat{\beta}_1(\lambda)\lambda^2 + \hat{\beta}_{-1}(\lambda)\lambda^{-2}, \\ T_{r\theta} &= T_{r\phi} = T_{\theta\phi} = 0. \end{aligned} \quad (9)$$

It follows that

$$T_{rr} - T_{\theta\theta} = \hat{\beta}_1(\lambda)(\lambda^{-4} - \lambda^2) + \hat{\beta}_{-1}(\lambda)(\lambda^4 - \lambda^{-2}). \quad (10)$$

Comparing Eq. (10) with Eq. (7), we conclude that

$$T_{rr} - T_{\theta\theta} = \lambda^{-2}f(\lambda^{-2} - 1; \alpha_1, \dots, \alpha_\ell). \quad (11)$$

We assume that the thick-walled spherical shell is at static equilibrium after the dilatation. At each place in the current configuration of the shell, the equations of equilibrium are satisfied. By Eq. (9), the only non-trivial equation of equilibrium can be simplified as

$$dT_{rr}/dr + 2(T_{rr} - T_{\theta\theta})/r = 0. \quad (12)$$

If the thick-walled shell is at equilibrium under an internal pressure p_i and outside pressure p_o , by integrating Eq. (12) we obtain the relation

$$\begin{aligned} p_i - p_o &= -2 \int_{r_i}^{r_o} r^{-1} (T_{rr} - T_{\theta\theta}) dr \\ &= -2 \int_{r_i}^{r_o} (\lambda^2 r)^{-1} f(\lambda^{-2} - 1; \alpha_1, \dots, \alpha_\ell) dr \\ &= 2 \int_{\lambda_1}^{\lambda_2} \lambda^{-3} (\lambda^3 - 1)^{-1} f(\lambda^{-2} - 1; \alpha_1, \dots, \alpha_\ell) d\lambda; \end{aligned} \quad (13)$$

where $\lambda = r/R$, $\lambda_1 = r_i/R_i$, and $\lambda_2 = r_o/R_o$. In deducing Eq. (13)₃ from Eq. (13)₂ we have used the assumption that the material of the thick-walled shell is incompressible.

Let us derive an approximation to Eq. (13) when the shell in question can be taken as thin, in which case we say that we are considering the dilatation of a spherical membrane. Suppose the membrane has thickness h_m and radius R_m when it is at its natural state. Let r_m be its radius after dilatation. By the assumption of incompressibility, after

dilatation the thickness of the membrane is

$$h \cong h_m \lambda_m^{-2}, \quad (14)$$

where $\lambda_m = r_m/R_m$. Let $k = h_m/R_m$ be the ratio of the original thickness and radius of the membrane. From Eq. (13)₂ we obtain the approximation

$$\begin{aligned} p_i - p_o &\cong -2h(r_m \lambda_m^2)^{-1} f(\lambda_m^{-2} - 1; \alpha_1, \dots, \alpha_\ell) \\ &\cong -2k \lambda_m^{-5} f(\lambda_m^{-2} - 1; \alpha_1, \dots, \alpha_\ell). \end{aligned} \quad (15)$$

Eq. (15) is useful in modelling the dilatation of the pericardium. Of course, the appropriate stress-strain relation should be used. Generally speaking, we expect that we can use Eq. (1) both for the pericardium and for the left ventricle. The elastic parameters, however, will assume different values for the two instances.

COMPARISON WITH EXPERIMENTAL DATA

We tested our model by using it to fit some experimental data in the literature. Before we could proceed, an explicit form of the function f in Eq. (1) must be given. The function form tried first was:

$$\sigma = \alpha(\exp(\beta\epsilon) - 1); \quad (16)$$

here α and β are the material parameters. Eq. (16) is known to give good fit to data of uniaxial tension tests for many soft biological tissues (see, e.g., Fung (1972) and references therein) and in particular for canine pericardium (cf. Rabkin and Hsu (1975)).[¶] Both α and β are positive in tension tests. Of course Eq. (16) need not be valid for compression tests. However, for the materials and the range of strain

[¶]We add two comments: (i) Eq. (16) has the drawback that the natural state must be specified to define ϵ . Experimentally the well-tested equation is in fact $d\sigma/d\epsilon = \beta(\sigma + \alpha)$, the form of which is independent of the reference configuration to define ϵ . In the fitting of data below, we shall make assumptions to the effect that the natural state in question will be specified. Thence Eq. (16) suits our present purpose well. (ii) The stress σ in the equation $d\sigma/d\epsilon = \beta(\sigma + \alpha)$ means Lagrangian stress for some authors (Fung (1972), Rabkin and Hsu (1975)) and Eulerian stress for others (see, e.g., Pinto and Fung (1973)). Considering the variability of data, the simplifications inherent in our model and the usual range of strain in its intended applications, we believe that in our present context distinction of Eulerian stress and Lagrangian stress in Eq. (16) is not that important. Taking σ as Lagrangian stress in Eq. (16) gave a slightly better fitting of the data to be discussed below. Throughout this paper, unless specified otherwise, the symbol σ denotes Lagrangian stress.

in question, if the stress-strain curve for compression is similar in shape to that for tension, then the function form Eq. (16) should remain valid, although we expect α and β to assume negative values because σ and ϵ are negative for compression. The preceding hypothesis has some empirical support in the instance of the dog pericardium. Cf. Fig. 5 of Hildebrandt et al. (1969a). Note in particular the two empirical formulae given in the figure for dog pericardium and the fact that $\epsilon = \lambda - 1$ for uniaxial tension tests and $\epsilon = \lambda^{-2} - 1$ for biaxial uniform-extension tests.

Pegram et al. (1975) studied changes in left ventricular internal diameter resulting from increasing intrapericardial pressure induced by increasing the pericardial fluid volume in closed chest, anaesthetized dogs. Their Fig. 2 includes a plot of change in pericardial end-diastolic diameter against change in pericardial pressure; each data-point in the plot is an average for six or seven dogs. The pericardial diameter at the control state (at which change in pericardial pressure = 0) is given in the last column of their Table 1. We used Eq. (15) with Eq. (16) for f to fit the aforementioned data of Pegram et al. In the fitting we assumed that p_o be constant; moreover, at the control state, $p_i = p_o$ and the pericardium be unstressed. Let Δp and Δd_m be the change in pericardial end-diastolic pressure and diameter, respectively. Under our assumptions $\Delta p = p_i - p_o$ in Eq. (15). Thence in our model Δp and Δd_m are related by

$$\Delta p = -2k\alpha\lambda_m^{-5}(\exp(\beta(\lambda_m^{-2} - 1)) - 1), \quad (17)$$

where $\lambda_m = 1 + (\Delta d_m / 2R_m)$. The parameters that can be determined from data of Δp against Δd_m are β and the product $k\alpha$. We determined the least squares estimates of $k\alpha$ and β from the data of Pegram et al. by nonlinear regression using IMSL subroutine ZXSSQ (a finite difference analogue of the Levenberg-Marquardt method). The results were as follows: $k\alpha = -0.509$ mm Hg, $\beta = -12.6$. Predictions from the model were close to the experimental values. See Table 1 and Fig. 1.

The computer output of the IMSL subroutine ZXSSQ includes also information from which approximate standard error and confidence intervals can be calculated for the estimated parameters. We calculated what follows: standard error of $k\alpha = 0.069$ mm Hg, standard error of $\beta = 0.572$; the Bonferroni joint confidence intervals at the 95% level were given by $k\alpha = (-0.509 \pm 0.186)$ mm Hg, and $\beta = -12.6 \pm 1.5$.

The calculation of the approximate standard errors and confidence intervals is based on a number of statistical assumptions. Whether those assumptions would be valid for the problem at hand is dubious. However, the standard errors and confidence intervals will at least provide an impression about the goodness of fit. Indeed, as we shall discuss below, such calculations led us to abandon a model based on a stress-strain relation proposed by Hildebrandt et al. (1969b), although it also gave good predictions.

The fitting above did not deliver an estimate for α . Vito (1979) reported an average thickness of 0.233 mm for twenty specimens of dog pericardium. Should we put $h_m = 0.233$ mm and $k \equiv h_m / R_m = 0.233 / 29.86$,

the estimated value of α would be equal to -65.2 mm Hg or -8.87×10^{-4} kg/mm². The absolute values $|\alpha| = 8.87 \times 10^{-4}$ kg/mm² and $|\beta| = 12.6$ fall in the range of values of α and β reported by Rabkin and Hsu (1975); they obtained those values from data of uniaxial tension tests on six specimens of canine pericardium. We should, however, caution that for a given specimen the absolute values $|\alpha|$ and $|\beta|$ for compression need not be equal to those for tension tests.

The paper of Pegram et al. (1975) did not include sufficient data for testing Eq. (13). Since we failed to find suitable data in the literature, we used the data of Spotnitz et al. (1966), which were obtained from 27 specimens of excised canine left ventricles. Our model is meant to describe the heart at end-diastole. Using pressure-volume data obtained under passive conditions is undesirable.

We used Eqs. (13) and (16) to fit the data of Spotnitz et al. In the fitting we assumed that the left ventricles be unstressed when the transmural pressure $p_i - p_o$ was null. We determined the least squares estimates of α and β by nonlinear regression, using IMSL subroutine ZXSSQ. We calculated also the standard errors and the 95% Bonferroni joint-confidence intervals for the estimated parameters. The results were as follows: $\alpha = -0.107$ mm Hg, $\beta = -13.1$; standard error of $\alpha = 0.026$ mm Hg, standard error of $\beta = 0.431$; the Bonferroni joint confidence intervals at the 95% level were given by $\alpha = (-0.107 \pm 0.075)$ mm Hg and $\beta = -13.1 \pm 1.2$. The model in question gave good predictions. See Table 2 and Fig. 2.

It is interesting to compare the two sets of values of α and β obtained above. The difference between the estimated values of β for the canine pericardium and left ventricle is statistically insignificant. Should the estimated average thickness of pericardium be sharp, the value of $|\alpha|$ for the pericardium would be at the 95% confidence level at least several hundred times larger than that for the left ventricle. In other words, while the stress-strain curves for uniaxial compression are similar in shape for the two materials, we expect the canine pericardium to be at least several hundred times stiffer than the muscle of the canine left ventricle. We should, however, caution that the two sets of values of α and β pertain to two different groups of specimens and the average thickness of canine pericardium is estimated from a third group.

For an incompressible and isotropic elastic material, the stress-strain relation Eq. (1) can be determined empirically through biaxial uniform-extension tests. Hildebrandt et al. (1969b) reported that the function

$$\sigma = K(\Lambda^3 - 1)/\Lambda^2(\Lambda - \Lambda_0)(\Lambda - \Lambda_{00}), \quad (18)$$

where K , Λ_0 , Λ_{00} are material parameters and $\Lambda \equiv 1 + \epsilon$ is the stretch ratio, gave good fit to experimental data of both uniaxial tension tests and uniform biaxial extension tests on several soft biological tissues. We attempted to fit the data of Pegram et al. in Table 1 above by using Eqs. (15) and (18). We followed the same fitting procedure used for Eq. (17).

While the least squares estimates of the material parameters did give predictions close to experimental data, two of the estimates had large variances and covariances. We believe that the large variances and covariances are due to over-parametrization with respect to fitting of the given data. In other words the given data will not suffice to give sharp estimates for all the three material parameters. Since we expected that the same phenomenon would occur if we used Eqs. (13) and (18) to fit the data of Spotnitz et al. given in Table 2 above, we did not proceed with the fitting.

In another paper Hildebrandt et al. (1969a) proposed a stress-strain relation specifically for biaxial uniform extensions of dog pericardium. The relation is

$$\sigma = -K\lambda^2(\lambda^2 - \lambda^{-4})(\lambda^{-2} - b)^{-1}; \quad (19)$$

here $\lambda^{-2} \equiv 1 + \epsilon$, K and b are material constants. (Cf. their Eqs. (10) and (11). Note that the symbol σ stands for Eulerian stress in the paper of Hildebrandt et al. (1969a), and it denotes Lagrangian stress here.) Eqs. (15) and (19) gave a good fit to the pericardium data of Pegram et al. (see Table 1 above). The least squares estimates were $Kk = 1.10$ mm Hg and $b = 0.652$, with standard errors equal to 0.09 mm Hg and 0.009 , respectively. The sum of squared residuals was 1.2 times of that which resulted when we used Eq. (17) to fit the pericardium data. Eqs. (13) and (19), however, were less satisfactory for fitting the data

of Spotnitz et al. as regards the canine left ventricle (see Table 2 above). While Eqs. (13) and (19) gave sharp estimates of the material parameters, the least squares estimates produced a sum of squared residuals almost ten times of that which resulted when Eqs. (13) and (16) were used.

In summary, among the three stress-strain relations considered, the "exponential law" Eq. (16) gave the best results. It is preferred for the stress-strain relation in our model.

DISCUSSION: APPLICATION TO INTACT MAN

Our model is meant to describe the left ventricle plus pericardium at end-diastole. It should be tested against pressure-volume data obtained from conscious or anaesthetized human beings. Procurement of requisite data is indeed possible.

The measurement of heart and pericardial volumes can be obtained noninvasively in man by the use of echocardiographic techniques. These methods utilize reflected sound waves to mark the inner and outer surfaces of the pericardium and myocardium. Although the estimate of myocardial volume is more accurate than pericardial volume, both measurements can be readily obtained. The measurement of ventricular volumes can be made precisely using invasive means. The insertion of a catheter into the heart from a vein or an artery permits the injection of a dye, which can be detected radiologically to enable the calculation of relevant volumes.

The measurement of pressure cannot be done noninvasively. Catheters must be inserted into the ventricles and the pericardial sac. The insertion of a catheter into the left or right ventricle is done daily in most major hospitals in selected individuals to diagnose heart disease. Insertion of a catheter into the pericardium is done only in patients who have sufficient fluid in the pericardial sac, for otherwise it may compromise the cardiovascular system. Albeit not a common occurrence, a number of investigations have utilized this method to measure pericardial pressure in man when fluid is being removed from the pericardial space. A recent study by Tyberg et al. (1986) has shown a high correlation between right atrial pressure and pericardial pressure, which may provide an important less invasive method to measure pericardial pressure.

Even with data obtained from procedures outlined above, a problem remains. In our modelling we have assumed that we know the inner and outer radii of the thick-walled shell, the thickness and radius of the spherical membrane when they are at ease. It is impossible to ascertain these numbers for a living subject by direct measurement. Even the natural length of a strip of excised pericardium or muscle specimen is difficult to determine. Perhaps we can avoid this problem by making reasonable approximations. For instance, for a normal man at rest, it may be a sufficiently good approximation to assume the pericardium as at ease at end-diastole. Indeed we have made a similar assumption when we use Eq. (17) to fit the data of Pegram et al. Perhaps our modelling may have

to be modified so that the natural states are no longer used as the reference configurations. A more complex model, however, will contain more parameters, which may lead to the problem of over-parametrization for the available data.

In summary, the present study has developed a model of the heart with pericardium, which fit well experimental data from canine heart and pericardium. Future studies should tackle the more difficult problems of refinement of the model and utilization of pressure-volume data from man.

ACKNOWLEDGMENT

We thank Mr. Quan-Xin Sun for helping us in the computer work. The research of P.N. Shivakumar was supported in part by the University of Manitoba Research Board under Grant No. 431-1709-80 and by the Natural Sciences and Engineering Research Council of Canada (NSERC) under Grant No. A7899. When the present work was initiated, C.-S. Man was Assistant Professor of Civil Engineering at The University of Manitoba. There his researches were supported by grants from NSERC. C.-S. Man did part of this research when he was a long-term visitor at the Institute for Mathematics and its Applications, University of Minnesota.

REFERENCES

- Demiray, H. (1976) Large deformation analysis of some basic problems in biophysics. Bull. Math. Biol. 38, 701-712.
- Fung, Y.-C. B. (1972) Stress-strain-history relations of soft tissues in simple elongation. Biomechanics: Its Foundations and Objectives (Edited by Fung, Y.C., Perrone, N., and Anliker, M.), pp. 181-208. Prentice-Hall, Englewood Cliffs.
- Glantz, S.A., Misbach, G.A., Moores, W.Y., Mathey, D.G., Lekven, J., Stowe, D.F., Parmley, W.W., and Tyberg, J.V. (1978) The pericardium substantially affects the left ventricular diastolic pressure-volume relationship in the dog. Circulation Research 42, 433-441.
- Hildebrandt, J., Fukaya, H., and Martin, C.J. (1969a) Stress-strain relations of tissue sheets undergoing uniform two-dimensional stretch. J. Appl. Physiol. 27, 758-762.
- Hildebrandt, J., Fukaya, H., and Martin, C.J. (1969b) Simple uniaxial and uniform biaxial deformation of nearly isotropic incompressible tissues. Biophys. J. 9, 781-791.
- Kanazawa, M., Shirato, K., Ishikawa, K., Nakajima, T., Haneda, T., and Takishima, T. (1983) The effect of pericardium on the end-systolic pressure-segment length relationship in canine left ventricle in acute volume overload. Circulation 68, 1290-1298.
- Mirsky, I. (1973) Ventricular and arterial wall stresses based on large deformation analyses. Biophys. J. 13, 1141-1159.
- Pegram, B.L., Kardon, M.B., and Bishop, V.S. (1975) Changes in left ventricular internal diameter with increasing pericardial pressure. Cardiovascular Research 9, 707-714.
- Pinto, J.G., and Fung, Y.C. (1973) Mechanical properties of the heart muscle in the passive state. J. Biomechanics 6, 597-616.

- Rabkin, S.W., and Hsu, P.H. (1975) Mathematical and mechanical modeling of stress-strain relationship of pericardium. Am. J. Physiol. 229, 896-900.
- Shirato, K., Shabetai, R., Bhargava, V., Franklin, D., and Ross, J. (1978) Alteration of the left ventricular diastolic pressure-segment length relation produced by the pericardium. Circulation 57, 1191-1198.
- Spotnitz, H.M., Sonnenblick, E.H., and Spiro, D. (1966) Relation of ultrastructure to function in the intact heart: sacramere structure relative to pressure volume curves of intact left ventricles of dog and cat. Circulation Research 18, 49-66.
- Truesdell, C., and Noll, W. (1965) The non-linear field theories of mechanics. Encyclopedia of Physics (Edited by S. Flügge), Vol. III/3, pp. 1-602. Springer-Verlag, Berlin.
- Tyberg, J.V., Taichman, G.C., Smith, E.R., Douglas, N.W.S., Smiseth, O.A., and Keon, W.J. (1986) The relationship between pericardial pressure and right atrial pressure: an intraoperative study. Circulation 73, 428-432.
- Vito, R.P. (1979) The role of the pericardium in cardiac mechanics. J. Biomechanics 12, 587-592. Corrections to the preceding paper published under the title "Response to the letter of H.A. Puryear and R.A. Casper" appeared in J. Biomechanics 13 (1980), p. 636.

Table 1. Comparison of predictions from Eq. (17) with experimental data given in Fig. 2(A) of Pegram et al.; Δd_m = change in pericardial end-diastolic diameter, Δp = change in pericardial end-diastolic pressure, $2R_m = 59.71$ mm, $k\alpha = -0.509$ mm Hg, $\beta = -12.6$.

Experimental Data		Prediction from Model
Δd_m (mm)	Δp (mm Hg)	Δp (mm Hg)
1.40	1.00	0.70
3.00	2.00	1.78
4.20	3.00	2.86
5.40	4.00	4.22
6.00	5.00	5.02
7.05	6.00	6.64
7.30	7.00	7.07
7.55	8.00	7.51
8.20	9.00	8.76
8.80	10.00	10.03
9.25	11.00	11.06

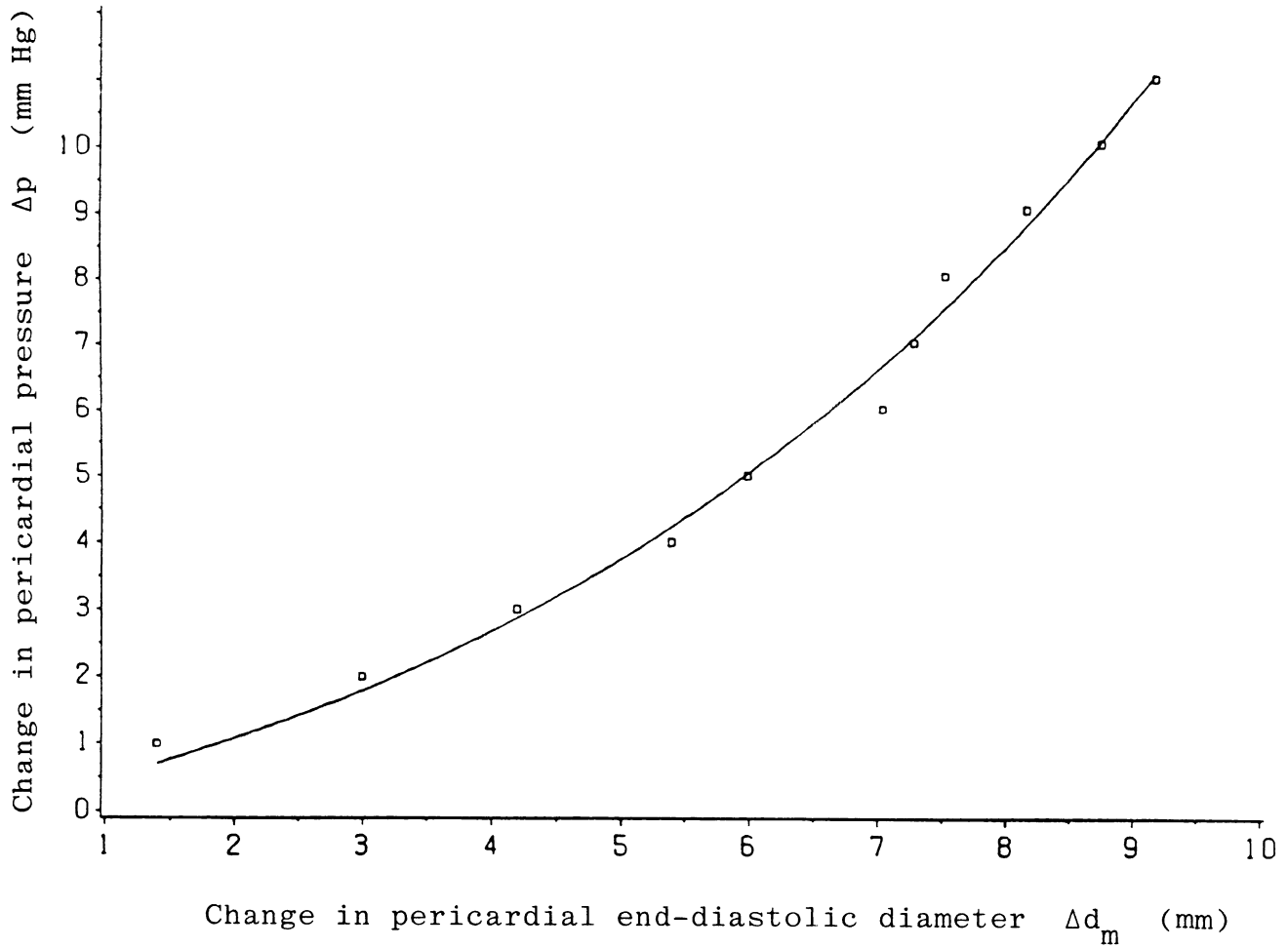


Fig. 1. Fitting canine pericardium data of Pegram et al. by using Eq. (17). Each \square denotes an experimental data-point. The solid curve pertains to parameters $k\alpha = -0.509$ mm Hg, $\beta = -12.6$.

Table 2. Comparison of predictions from Eqs. (13) and (16) with experimental data given in Table 1 of Spotnitz et al.; $R_i = 14.4$ mm, $R_o = 29.6$ mm, $\alpha = -0.107$ mm Hg, $\beta = -13.1$. The last row of data is obtained by taking averages of data given in the two rows with $p_i - p_o$ estimated as 30+ mm Hg in the paper of Spotnitz et al.

Experimental Data			Prediction from Model
r_i (mm)	r_o (mm)	$P_i - P_o$ (mm Hg)	$P_i - P_o$ (mm Hg)
18.2	30.7	2.0	1.6
19.3	31.1	3.0	2.9
19.8	31.3	3.0	3.7
20.5	31.7	5.0	5.0
22.7	32.7	10.0	10.8
23.3	32.9	12.0	12.9
23.9	33.2	15.0	15.1
24.6	33.6	20.0	17.8
27.5	35.2	30.0	30.6

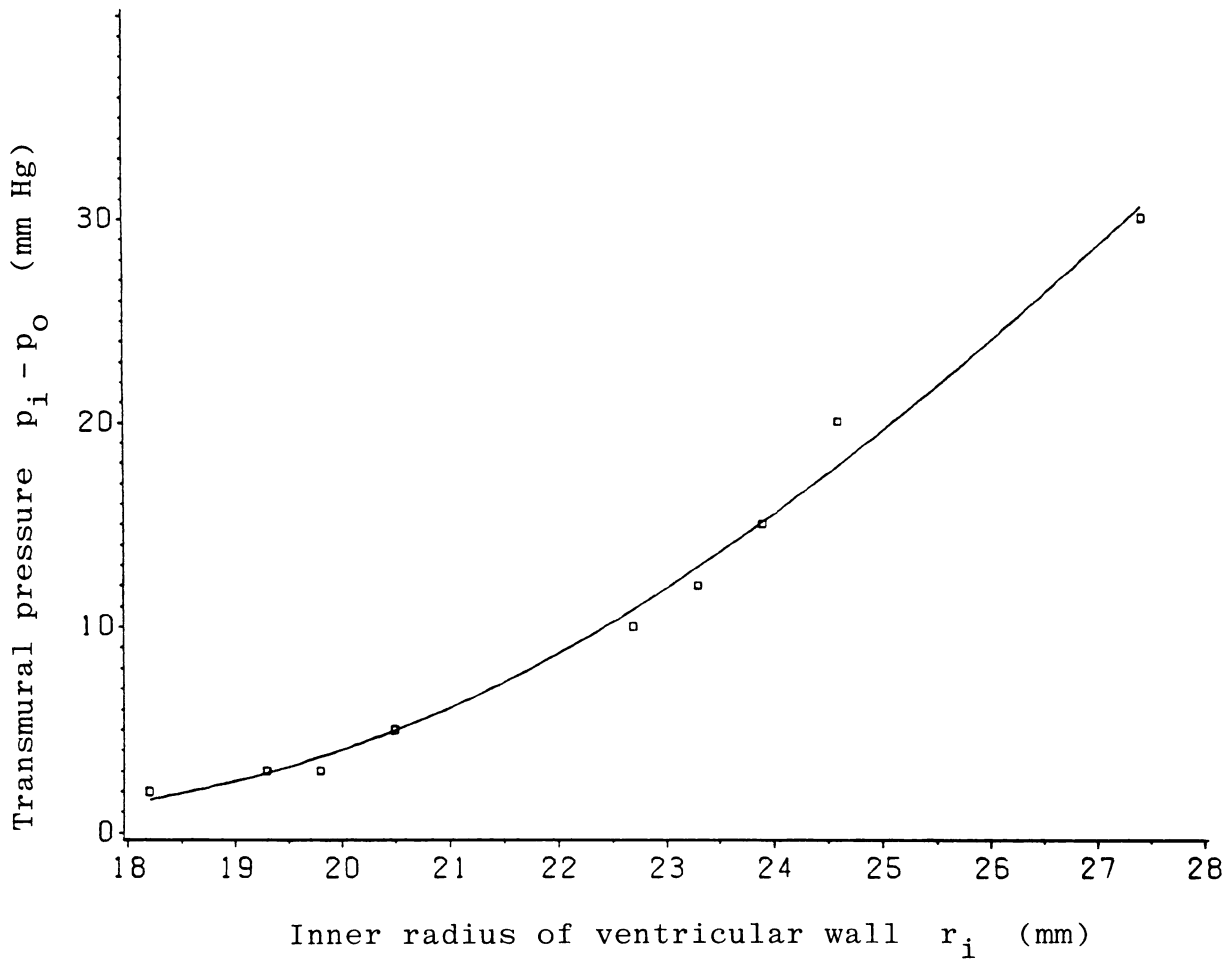


Fig. 2. Fitting canine left-ventricular data of Spotnitz et al. by using Eqs. (13) and (16). Each \square denotes an experimental data-point. The solid curve pertains to parameters $\alpha = -0.107$ mm Hg, $\beta = -13.1$.